nature plants

ARTICLES

PUBLISHED: 26 JUNE 2017 | VOLUME: 3 | ARTICLE NUMBER: 17087

The evening complex coordinates environmental and endogenous signals in *Arabidopsis*

Daphne Ezer[1], Jae-Hoon Jung[1], Hui Lan[1], Surojit Biswas[1†], Laura Gregoire[2], Mathew S. Box[1], Varodom Charoensawan[1,3], Sandra Cortijo[1], Xuelei Lai[1,2], Dorothee Stöckle[1], Chloe Zubieta[2], Katja E. Jaeger[1] and Philip A. Wigge[1*]

Plants maximize their fitness by adjusting their growth and development in response to signals such as light and temperature. The circadian clock provides a mechanism for plants to anticipate events such as sunrise and adjust their transcriptional programmes. However, the underlying mechanisms by which plants coordinate environmental signals with endogenous pathways are not fully understood. Using RNA-sequencing and chromatin immunoprecipitation sequencing experiments, we show that the evening complex (EC) of the circadian clock plays a major role in directly coordinating the expression of hundreds of key regulators of photosynthesis, the circadian clock, phytohormone signalling, growth and response to the environment. We find that the ability of the EC to bind targets genome-wide depends on temperature. In addition, co-occurrence of phytochrome B (phyB) at multiple sites where the EC is bound provides a mechanism for integrating environmental information. Hence, our results show that the EC plays a central role in coordinating endogenous and environmental signals in *Arabidopsis*.

Plants are sensitive to their environment, and the distribution and phenology of plants has already altered in response to climate change[1,2]. Such growth and developmental changes require the integration of multiple environmental signals, such as light and temperature, into endogenous gene expression programmes. The circadian clock plays a key role in this process by enabling plants to anticipate future events such as sunrise and darkness as well as gating responses to environmental information according to time of day[3–5]. The expression levels of many circadian clock genes vary in response to changes in the environment[6], but the underlying mechanisms by which these signals are integrated are not known. The circadian clock in *Arabidopsis* contains multiple interlocking loops with transcriptional and post-translational regulation. Three circadian clock genes, *EARLY FLOWERING3, 4 (ELF3 and 4)* and the MYB transcription factor *LUX ARRYTHMO (LUX)* together comprise the evening complex (EC)[5,7], and are expressed at the end of the day. The EC coordinates elongation growth in *Arabidopsis* seedlings, as it directly represses the expression of the bHLH transcription factor *PHYTOCHROME INTERACTING FACTOR 4 (PIF4)* (refs 7–9). *PIF4* is necessary for warm temperature-mediated elongation growth[10], and *pif4* and *pif4,5* mutants also display a reduced induction of flowering in response to warm temperature[11–14]. Natural variation in the activity of the EC is responsible for differences in thermal responsiveness and warmer temperatures reduce the binding of the EC to target promoters, resulting in increased *PIF4* expression[15,16].

Of the core EC components, only LUX is recognisable as a transcription factor and has been shown to have direct DNA binding activity[17], suggesting that the genome-wide targeting of the EC is likely dependent on the cognate LUX Binding Sites (LBS). Indeed, it has been shown that several known targets of LUX possess LBS in their promoters where binding of LUX has been demonstrated using chromatin immunoprecipitation (ChIP)[7,17,18].

Although the role of the EC has been studied at specific circadian loci, the system-wide impact of the EC is not known, since its global binding pattern and regulatory effects are not yet characterized. In addition, the mechanisms by which the EC is able to provide environmental responsiveness to target loci and integrate environmental signals into the circadian clock are poorly understood. In this study, we demonstrate that the EC regulates key nodes controlling photosynthesis, the circadian clock, growth, phytohormones and temperature signals. We show that the EC directly integrates temperature information and we describe a mechanism by which the cobinding of phytochrome B (phyB) with the EC to target loci enables environmental signals to be directly integrated into the circadian clock.

Results

G-box (CACGTG) motifs are highly enriched at EC binding sites. To understand how the EC may control plant responses to the environment, we sought to determine its binding genome-wide. Although the LBS is found at more than 10,000 sites in the *Arabidopsis* genome, typically only a subset of the theoretical transcription factor binding sites are occupied *in vivo*. It is also not known to what extent the target sites of the separate EC proteins overlap genome-wide. To resolve these questions we mapped the LUX, ELF3 and ELF4 target sites *in vivo* using ChIP coupled to sequencing (ChIP-seq) using epitope tagged versions of these genes expressed under their own promoters (see Supplementary Fig. 1 for westerns, Supplementary Fig. 2 for complementation and Supplementary Table 1 for sequencing read counts).

In the early evening (Zeitgeber Time (ZT) 10, 2 h after darkness) at 22 °C, there is a large overlap in the binding sites of LUX, ELF4 and ELF3 (Fig. 1a,b and Supplementary Fig. 3 and Supplementary Table 2). Additionally, the LUX ChIP at 22 °C has fewer significant binding sites than the other EC components, with 42 peaks being detected for LUX at 22 °C, compared to 182 for ELF3 (Fig. 1b).

[1]Sainsbury Laboratory, University of Cambridge, 47 Bateman Street, Cambridge CB2 1LR, UK. [2]LPCV, CNRS, CEA, INRA, Univ. Grenoble Alpes, BIG, 38000 Grenoble, France. [3]Department of Biochemistry, Faculty of Science, and Integrative Computational BioScience (ICBS) Center, Mahidol University, Bangkok 10400, Thailand. †Present address: Division of Medical Sciences, Harvard Medical School, Boston, Massachusetts 02115, USA.
*e-mail: philip.wigge@slcu.cam.ac.uk

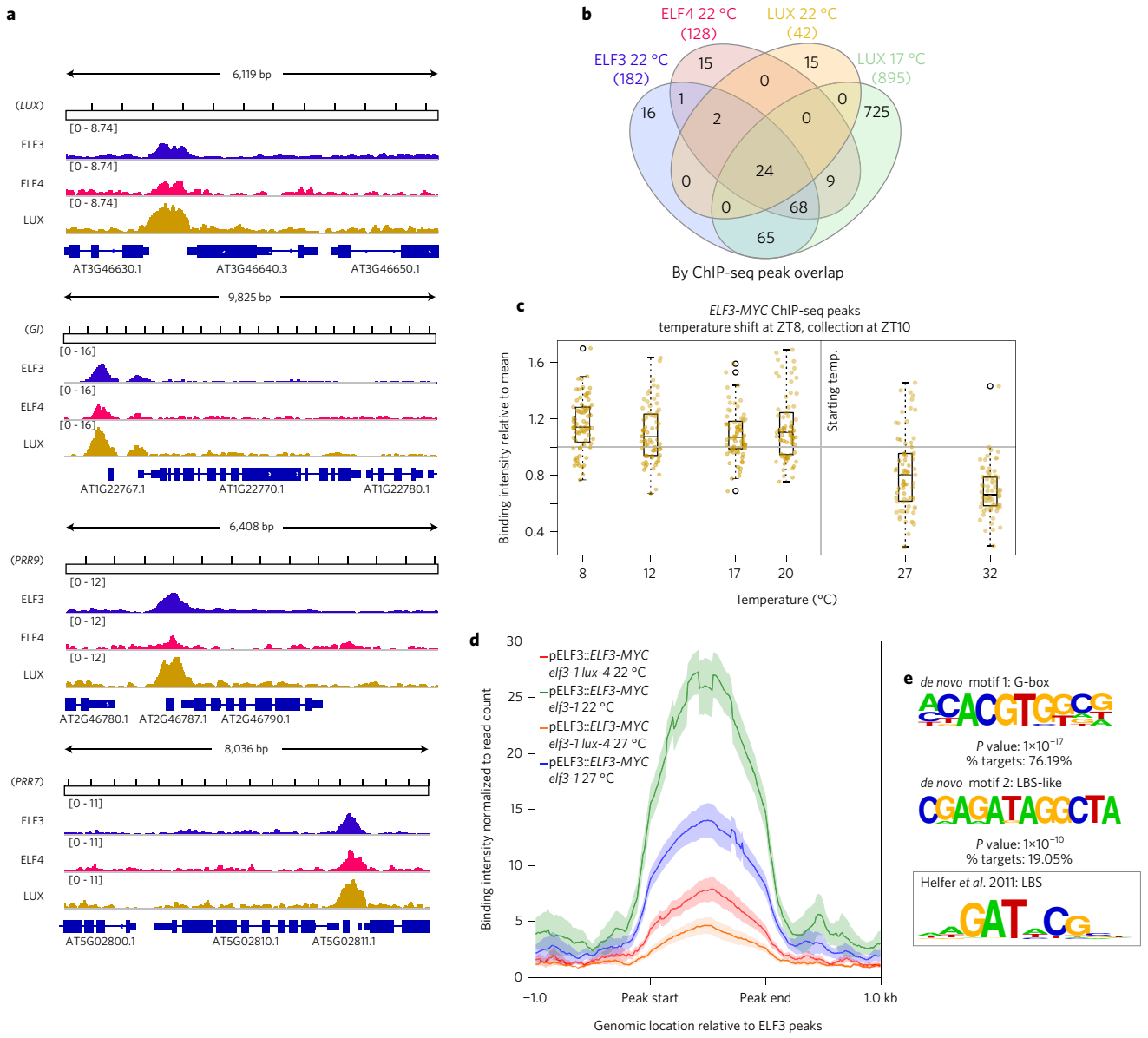

Figure 1 | There is a high degree of overlap of binding sites for ELF3, ELF4 and LUX genome-wide. a, ELF3, ELF4 and LUX all bind to the same positions near key circadian targets, such as *PRR9, GI* and *LUX*. **b**, Venn diagrams showing the degree of ChIP-seq peak overlap of ELF3, ELF4 and LUX at 22 °C and LUX at 17 °C collected from SD grown seedlings at ZT10 (2 h of darkness). Note that the LUX at 17 °C data is also shown in Supplementary Fig. 1a,b. The total number of peaks is shown in parentheses. Note that the numbers in each oval are smaller than those in parentheses, because there are a number of cases where two peaks from one ChIP-seq overlap with a single peak from another ChIP-seq, but this will only be counted as a single overlap event in the Venn diagram (see Methods for more details). **c**, Plants were grown in SD conditions at 22 °C until ZT8 and then shifted to a range of temperatures. *ELF3-MYC* ChIP-seqs were conducted at ZT10. Binding intensity is calculated by MACS2 and for each peak the values were normalized by the average binding intensity of that peak across all temperature-shift experiments. **d**, The binding intensity profiles, as calculated by deeptools, are shown here for *ELF3-MYC* ChIP-seqs in *elf3-1* and *elf3-1/lux-4* backgrounds, at 22 °C and 27 °C. **e**, *De novo* motifs under LUX peaks at 22 °C were identified using Homer2—the first motif includes a G-box and the second motif appears similar to the LBS[17], with the exception that one C is replaced by a G (AGATAGG instead of AGATACG).

The reduced number of LUX peaks may be due to ELF3/ELF4 binding independently of LUX, or it may reflect a reduced detection resulting from a lower LUX ChIP efficiency.

To distinguish between these two possibilities, we sought to perform ChIP under conditions that would maximize the stability of LUX binding to improve the ChIP efficiency. Since it has been shown that the binding of EC components (ELF3 and ELF4) to the promoters of *PIF4, LUX* and *PRR9* decreases with warmer temperature[15], we performed an additional LUX ChIP-seq experiment at constant 17 °C (also at ZT10) to determine if additional targets could be identified. These experiments considerably increased the list of detectable LBS (Fig. 1b, Supplementary Table 2). These additional LUX peaks at 17 °C overlapped even more substantially with the ELF3 and ELF4 peaks at 22 °C: for example, 92% of ELF3 binding sites now overlap with other EC components. Since there are expected to be over 60,000 non-overlapping accessible regions for transcription factor binding in the *Arabidopsis* genome[19], this is a highly significant overlap (see 'VennDiagramStats' in Supplementary Table 3). These results are consistent with LUX binding to most if not all EC targets.

To determine whether the strength of binding of LUX changes globally in response to warmer temperatures, seedlings grown at 17 °C were shifted to 27 °C at ZT8 and collected at ZT9 and ZT10 (Supplementary Fig. 3a). The strength of the LUX binding

signal was weaker at the higher temperature at both time points (Supplementary Fig. 3b), consistent with previous observations showing ELF3 binding to target loci decreases at 27 °C (ref. 15).

We next analysed ELF3 binding to its targets in plants grown at 22 °C until ZT8 (dusk) and then shifted to a range of temperatures from 8 to 32 °C and measured at ZT10. There is a strong decline in ELF3 binding strength with increasing temperature across this range (Fig. 1c), consistent with previous observations that binding of ELF3 and ELF4 is temperature dependent. LUX has been shown to provide DNA binding specificity for the EC at a number of loci, and we observe a large global reduction in ELF3 occupancy in the *lux-4* background, confirming the importance of LUX in recruiting ELF3 to target loci (Fig. 1d). Interestingly, ELF3 binding is still highly responsive to temperature in *lux-4*, consistent with a role for ELF3 in responding to temperature (Fig. 1d).

Finally, we wished to determine whether LUX and ELF3 binding were consistent across multiple time points. Two additional LUX ChIP-seq experiments were conducted at 22 °C immediately before darkness (ZT8) and 4 h after darkness (ZT12), to complement the previous ChIP-seq data at ZT10 (Supplementary Fig. 3c). In addition, a time course ChIP-seq experiment was conducted for ELF3 with samples collected every 4 h for a 24 h cycle at 22 °C (Supplementary Fig. 3d). These results suggest that LUX binding at ZT8 and ZT10, the two time points with greatest *LUX* expression, are very similar; however, there is a reduction in binding at ZT12 (Supplementary Fig. 3c). Similarly, ELF3 binding near EC targets is high at dusk and in the early night (ZT8 to ZT16), with a reduction in binding during the day (Supplementary Fig. 3d). This pattern of binding intensity is consistent with the expression patterns for *LUX* and *ELF3*, suggesting that their binding strength correlates with transcript and protein levels.

These results indicate that *in vivo* LUX mostly binds in complex with other EC components in the early evening. However, we also observed strong LUX binding to many of the same binding sites in an *elf3-1* background, indicating that LUX binding *in vivo* can occur genome-wide independently of ELF3 (Supplementary Fig. 4). This is in agreement with *in vitro* studies showing the ability of LUX to bind targets is independent of ELF3 and ELF4 (Silva *et al.* under submission).

De novo motif analysis revealed two enriched elements under LBS at 22 °C at ZT10. Firstly, as expected, many peaks contain either perfect LBS sequences[17] or a motif with strong similarity to it, motif 2 (Fig. 1e). Interestingly, G-boxes are even more enriched, being found in 76% of LBS at 22 °C, ZT10 (Fig. 1e, Supplementary Table 4), including in the promoters of many different circadian clock genes, such as *CCA1, GI* and *PRR7* and *9*. This suggests that one or more G-box binding transcription factors may play a significant role in EC regulation and function. *De novo* motif analysis was also conducted for the other datasets, and is available in Supplementary Table 4 and Supplementary Fig. 5—in all cases the G-box was the most enriched motif. We observe that the G-boxes lie near the centre of the EC peaks, and the data obtained by DNA affinity purification sequencing[20] indicates multiple bZIP and bHLH transcription factors (TFs) as candidates for cobinding with the EC (Supplementary Fig. 6).

The EC is a node regulating photosynthesis, light, hormone, circadian and temperature signalling. Since the EC has been proposed to act as a transcriptional regulator, we sought to identify the functional targets of the EC: genes that are both bound by EC components and also show a transcriptional response in EC mutant backgrounds. As the EC regulates transcription in a diurnal fashion, we performed a gene expression time-course experiment, sampling every 4 h over a 24 h short day cycle (Supplementary Table 5). Because the EC has been shown to integrate temperature information[8,15,21], we performed this analysis at both 22 °C and 27 °C.

This enabled us to identify a set of genes present within 3,000 bp of an EC binding peak that also show differential expression in at least one time point in either the *elf3-1* or *lux-4* backgrounds compared to Col-0 (Table 1, Supplementary Table 6). This set of functional target genes for each EC component shows even more overlap with each other than do the original ChIP-seq peaks themselves, indicating the validity of this approach (Fig. 2a). Each gene referred to in the rest of the text as a potential 'EC target' has perturbed expression in at least one time point in *elf3-1* or *lux-4* and has at least two EC components binding within 3,000 bp as determined by ChIP-seq.

Next, we searched for enrichment of the *cis*-elements already identified (Fig. 2b, Supplementary Table 4) in ChIP-seq peaks in the vicinity of the functional targets. Interestingly, we observed an increase in the frequency of sequences corresponding to the true LBS, which are now more enriched than the related motif 2, suggesting that the true LBS is more important for a functional EC binding event compared to motif 2 (Fig. 2b). Additionally, we see that the occurrence of perfect G-boxes is increased in the subset of binding sites near EC functional targets. Together, these results suggest that functional EC binding is enriched for the co-occurrence of both LBS and G-box motifs; see Supplementary Fig. 6 and Supplementary Table 3. Furthermore, we wished to determine whether G-boxes were truly enriched under the EC peaks or whether they were simply enriched in the promoters of EC gene targets. We could find very few instances of G-boxes flanking our EC peaks (Supplementary Table 3), which suggests that these G-boxes are in fact enriched under the EC peaks. Such a combinatorial requirement is likely to contribute to the specificity of EC action genome-wide.

The EC is established as a regulator of circadian responses, particularly growth, and we observe the described binding of EC components to the promoters of *PRR9, LUX, PIF4* and *PIF5* (refs 7, 17, 18) (Table 1, Supplementary Figs 7 and 8). Additionally, there is extensive interaction between the EC and other clock master regulators, including *GI*, *CCA1* and *PRR7*, highlighting the high degree of cross-talk within the loops of the circadian clock[22]. Also, the EC appears to target a number of genes related to environment-dependent signalling and growth. In fact, most enriched gene ontology (GO) terms amongst the EC targets are for genes involved in photosynthesis (Supplementary Table 7, Supplementary Fig. 8), including many photosystem light harvesting proteins and chlorophyll A/B binding proteins. In addition to altering the expression of nuclear encoded chloroplast genes, the EC also binds to the promoter of *GUN5*, which is necessary for retrograde signalling from the chloroplast to the nucleus[23]. Large-scale shutdown of photosynthesis genes upon the onset of darkness (as in Supplementary Fig. 8) is presumably adaptive. Since the EC is not active in late night, these genes can then be reactivated before dawn in anticipation of light and photosynthesis. In addition to the described targets *PIF4* and *PIF5,* the EC binds the promoters of other light signalling genes such as *EARLY LIGHT INDUCIBLE PROTEIN* and *EARLY PHYTOCHROME RESPONSIVE1*.

In addition to the enrichment in photosynthesis and light response genes, the EC may regulate a number of genes implicated in heat response such as *DNAJ11* and *CXIP1* (see Supplementary Fig. 8), which protect against oxidative damage caused by heat stress[24] and the cold response (*CBF1,2,3* and *DREB2* class genes). Previously it has been shown that the promoter of *LUX* is bound by the master regulator of the cold response, CBF1 (ref. 25), suggesting that the EC and CBFs form a self-regulating loop.

Finally, a major role of the EC is to gate growth, and this has been connected to the regulation of *PIF4* and *5*, master regulators of the elongation response. Additionally, we observe extensive binding of

Table 1 | Evening complex gene targets.

Name	TAIR ID	Function	Reference
Photosynthesis and chloroplast function			
LHCA1	AT3G54890	A component of the light harvesting complex associated with photosystem I.	Jansson *et al.*, 1999[52]
PIF5	AT3G59060	A Myc-related bHLH transcription factor, which physically associated with APRR1/TOC1 and is a member of PIF3 TF family. Involved in shade avoidance. Functions as negative regulator of phyB. Protein levels are modulated by phyB.	Hornitschek *et al.*, 2012[53]
CAB1,2,3	AT1G29930 AT1G29920 AT1G29910	Member of Chlorophyll a/b-binding protein family.	Mitra *et al.*, 1989[54]
GUN5	AT5G13630	Encodes magnesium chelatase involved in plastid-to-nucleus signal transduction.	
CRB	AT1G09340	Encodes CHLOROPLAST RNA BINDING (CRB), a putative RNA-binding protein. CRB is important for the proper functioning of the chloroplast. Mutations in CRB also affect the circadian system, altering the expression of both oscillator and output genes.	Beligni, 2008[55]
Circadian clock			
GI	AT1G22770	Regulates several developmental processes, including photoperiod-mediated flowering, phyB signalling, circadian clock, carbohydrate metabolism and cold stress response.	Park *et al.*, 1999[56]
PRR7,9	AT5G02810 AT2G46790	PRR7 and PRR9 are partially redundant essential components of a temperature-sensitive circadian system.	Salome and McClung, 2005[57]
CCA1	AT2G46830	CCA1 and LHY function synergistically in regulating circadian rhythms of *Arabidopsis*.	Salome *et al.*, 2010[58]
LUX	AT3G46640	Encodes a myb family transcription factor with a single Myb DNA-binding domain (type SHAQKYF) that is unique to plants and is essential for circadian rhythms, specifically for transcriptional regulation within the circadian clock. LUX is required for normal rhythmic expression of multiple clock outputs in both constant light and darkness. It is coregulated with *TOC1* and seems to be repressed by CCA1 and LHY by direct binding of these proteins to the evening element in the *LUX* promoter.	Nusinow *et al.*, 2011[7]
AMY3	AT1G69830	Encodes a plastid-localized a-amylase. Expression is reduced in the *sex4* mutant. Loss of function mutations show normal diurnal pattern of starch accumulation/degradation. Expression follows circadian rhythms.	Seung *et al.*, 2013[59]
CDF1	AT5G62430	Dof-type zinc-finger domain-containing protein, similar to H-protein promoter binding factor-2a GI:3386546 from (*Arabidopsis thaliana*). Represses expression of CONSTANS (*CO*), a circadian regulator of flowering time. Interacts with LKP2 and FKF1. Expression oscillates under constant light conditions. Mainly expressed in the vasculature of cotyledons, leaves and hypocotyls, but also in stomata. Localized to the nucleus and acts as a repressor of *CO* through binding to the Dof binding sites in the *CO* promoter. Protein gets degraded by FKF1 in the afternoon.	Seaton *et al.*, 2015[60]
CDF 2,3	AT5G39660 AT3G47500	Dof-type zinc-finger domain-containing protein, identical to H-protein promoter binding factor-2a GI:3386546 from (*A. thaliana*). Interacts with LKP2 and FKF1, but its overexpression does not change flowering time under short- or long-day conditions.	Seaton *et al.*, 2015[60]
Temperature response			
CBF1,2,3	AT4G25490 AT4G25470 AT4G25480	Induces *COR* (cold-regulated) gene expression increasing plant freezing tolerance.	Jaglo-Ottosen *et al.*, 1999[61]
DREBA2	AT2G40350 AT2G40340	A member of the DREB subfamily A-2 of ERF/AP2 transcription factor family. DREB2A AND DREB2B are involved in response to drought.	Riechmann *et al.*, 2000[62]
DNAJ	AT4G36040	Chaperone DnaJ-domain superfamily protein; functions in: heat shock protein binding.	Chen *et al.*, 2010[63]
Growth			
PIF4	AT2G43010	Involved in shade avoidance response. Protein abundance is negatively regulated by phyB.	Koini *et al.*, 2009[10]
DOG1	AT5G45830	A quantitative trait locus involved in the control of seed dormancy.	Kendal *et al.*, 2011[64]
BNQ1,2	AT5G39860 AT5G15160	Required for appropriate regulation of flowering time.	Wang *et al.*, 2009[65]
BBX24	AT1G06040	BBX24 colocalizes with COP1 and plays a role in light signalling	Crocco *et al.*, 2015[66]
BBX22	AT1G78600	Light-regulated zinc-finger protein 1 (LZF1).	Gangappa *et al.*, 2013[67]
Phytohormone and light signalling			
AtCKX6	AT1G75450	Encodes a protein whose sequence is similar to cytokinin oxidase/dehydrogenase, which catalyses the degradation of cytokinins.	Bartrina *et al.*, 2011[68]
CRF4	AT4G27950	Encodes a member of the ERF (ethylene response factor) subfamily B-5 of ERF/AP2 transcription factor family.	Zwack *et al.*, 2015[69]
CRF5	AT2G46310	*CRF5* encodes one of the six cytokinin response factors. It is transcriptionally upregulated in response to cytokinin. CRF proteins rapidly relocalize to the nucleus in response to cytokinin. Analysis of loss-of-function mutants revealed that the CRFs function redundantly to regulate the development of embryos, cotyledons and leaves.	Cutcliffe *et al.*, 2011[70]
ARR6	AT5G62920	Encodes a Type-A response regulator that is responsive to cytokinin treatment. Its C-terminal domain is very short in comparison to other *Arabidopsis* ARRs (17 total). ARR6 protein is stabilized by cytokinin.	Zwack *et al.*, 2016[71]
ARR7	AT1G19050	Encodes a member of the *Arabidopsis* response regulator (ARR) family, most closely related to ARR15. A two-component response regulator protein containing a phosphate accepting domain in the receiver domain but lacking a DNA binding domain in the output. Involved in response to cytokinin and meristem stem cell maintenance. ARR7 protein is stabilized by cytokinin.	Wilson *et al.*, 2016[72]
RVE1	AT5G17300	Myb-like transcription factor that regulates hypocotyl growth by regulating free auxin levels in a time-of-day specific manner.	Rawat *et al.*, 2009[73]
CYP707A2	AT2G29090	Encodes a protein with ABA 8′-hydroxylase activity, involved in ABA catabolism. Member of the *CYP707A* gene family. This gene predominantly accumulates in dry seeds and is upregulated immediately following imbibition.	Dong *et al.*, 2014[74]
ELIP1	AT3G22840	Encodes a light-inducible protein.	Rizza, 2011[75]
RVE7	AT1G18330	Early phytochrome-responsive gene.	Li *et al.*, 2011[76]

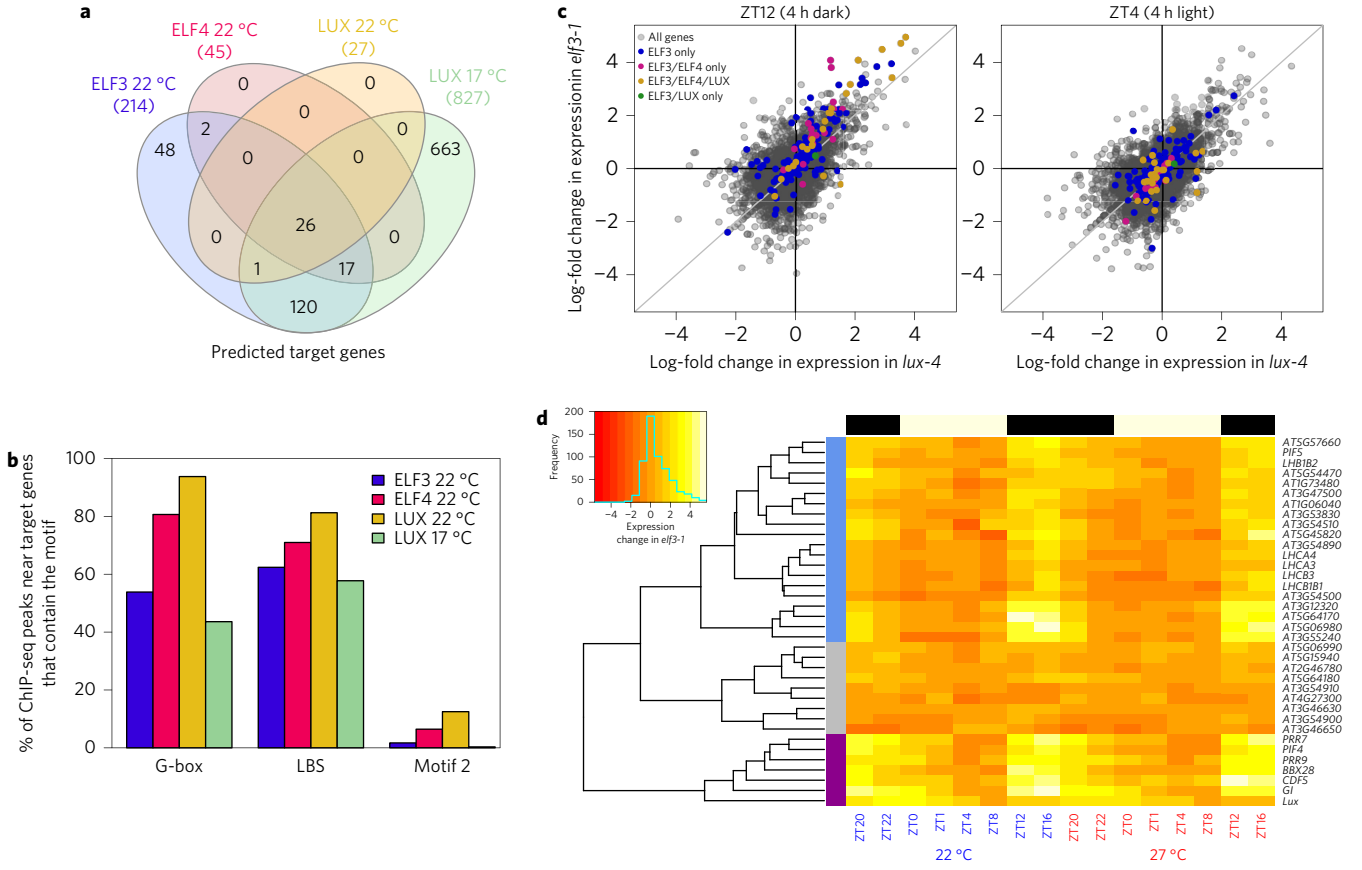

Figure 2 | The EC regulates a wide set of target genes controlling major biological processes in the plant, particularly the circadian clock, photosynthesis, temperature signalling, growth and phytohormone signalling. Target genes were identified for each EC component as being within 3,000 bp of a ChIP-seq peak and being differentially expressed in at least one time point in either *elf3-1* or *lux-4*. **a**, Degree of overlap between these gene targets. **b**, Among peaks that were within 3,000 bp of predicted gene targets, the proportion containing the motifs displayed in Fig. 1c: G-boxes (motif #1 in the *de novo* analysis), LBS[18] and motif #2. **c**, Gene expression values were normalized to TPM. The log-fold change in gene expression—that is, $\ln(TPM_{mutant}/TPM_{Col\text{-}0})$ at 22 °C for *elf3-1* and *lux-4* are compared to one another, both in the early evening, when the EC complex is present, and in the day, when the EC complex is absent. All genes that are among the top 5% most differentially expressed genes in at least one time point in either *elf3-1* or *lux-4* are shown in grey. Predicted target genes for ELF3, ELF4 or LUX at 22 °C are highlighted. **d**, Hierarchical clustering was conducted on the log-fold change (also the natural log) in expression in elf3-1 versus Col-0 at 22 °C for the predicted targets of ELF4 at 22 °C (blue text) and 27 °C (red text)—each row represents a gene, with all PIFs, light harvesting genes and circadian clock genes labelled by common name, and each column represents an RNA-sequencing sample. The bar above the clustering plot demonstrated the day/night cycle—the seedlings were grown in SD conditions. The clusters are designated by the purple, grey and blue sidebars.

the EC to a number of targets involved in controlling phytohormone signalling—such as the bHLH growth regulators *BANQUO1* and *2* that function downstream of the brassinosteroid responsive transcription factor BZR1 (refs 26 and 27) and the Myb-like transcription factor *REVEILLE1*, which controls free auxin levels[28]. Recently, it has been shown that plants deficient in cytokinins are hypersensitive to circadian stress[29]. Interestingly, we see extensive connections between the EC and cytokinin signalling, since the EC represses the genes *ARR6, ARR7, CYTOKINE OXIDASE5, CRF4* and *CRF5*.

Crucially, almost all of the proposed target genes show elevated levels of expression in *elf3-1* and *lux-4* in the early evening, but not the day, which is consistent with the EC's role as an early evening repressor (Fig. 2d, Supplementary Figs 8–10, see "Scatterplots Stats" in Supplementary Table 3 for *P* value calculations). To further understand the temporal dynamics of these EC targets, the ELF4 targets were clustered based on the log-fold change of expression in *elf3-1* (Fig. 2d) (ELF4 targets were chosen as these have the largest degree of overlap with ELF3 and LUX, making them by this measure the best predictor of EC presence). Three clusters emerged—the largest cluster (shown in blue, which included *PIF5* and many members of the photoharvesting system) had increased expression in the early evening. A second cluster (shown in purple)—which included all of the key circadian targets as well as *PIF4*—had increased expression in *elf3-1* in the early morning, as well as at night. The last cluster had no clear pattern of expression in *elf3-1*, and may include genes that are 'false-positive' candidates. However, this third cluster (grey) contains only nine genes, suggesting that we have successfully identified a high-quality list of global EC gene targets.

About 40 of the direct targets of the EC are transcription factors, suggesting that the EC is a major node regulating large-scale transcriptional responses in the cell. For LUX at 17 °C, the GO term "transcription, DNA-regulated" is enriched (PANTHER, *P* value 4.98E-09). Consistent with this, in *elf3-1* and *lux-4* we observed large-scale perturbation to the transcriptome extending beyond the evening period when the EC is most active. Many of these genes misregulated in *elf3-1* and *lux-4* are not bound by the EC, indicating that they are instead indirect targets (Supplementary Fig. 11).

ELF3 and LUX are both required for EC repression of circadian targets. Because of the critical role the EC plays in controlling the circadian clock, we decided to further investigate the expression pattern of the cluster composed mainly of circadian genes from

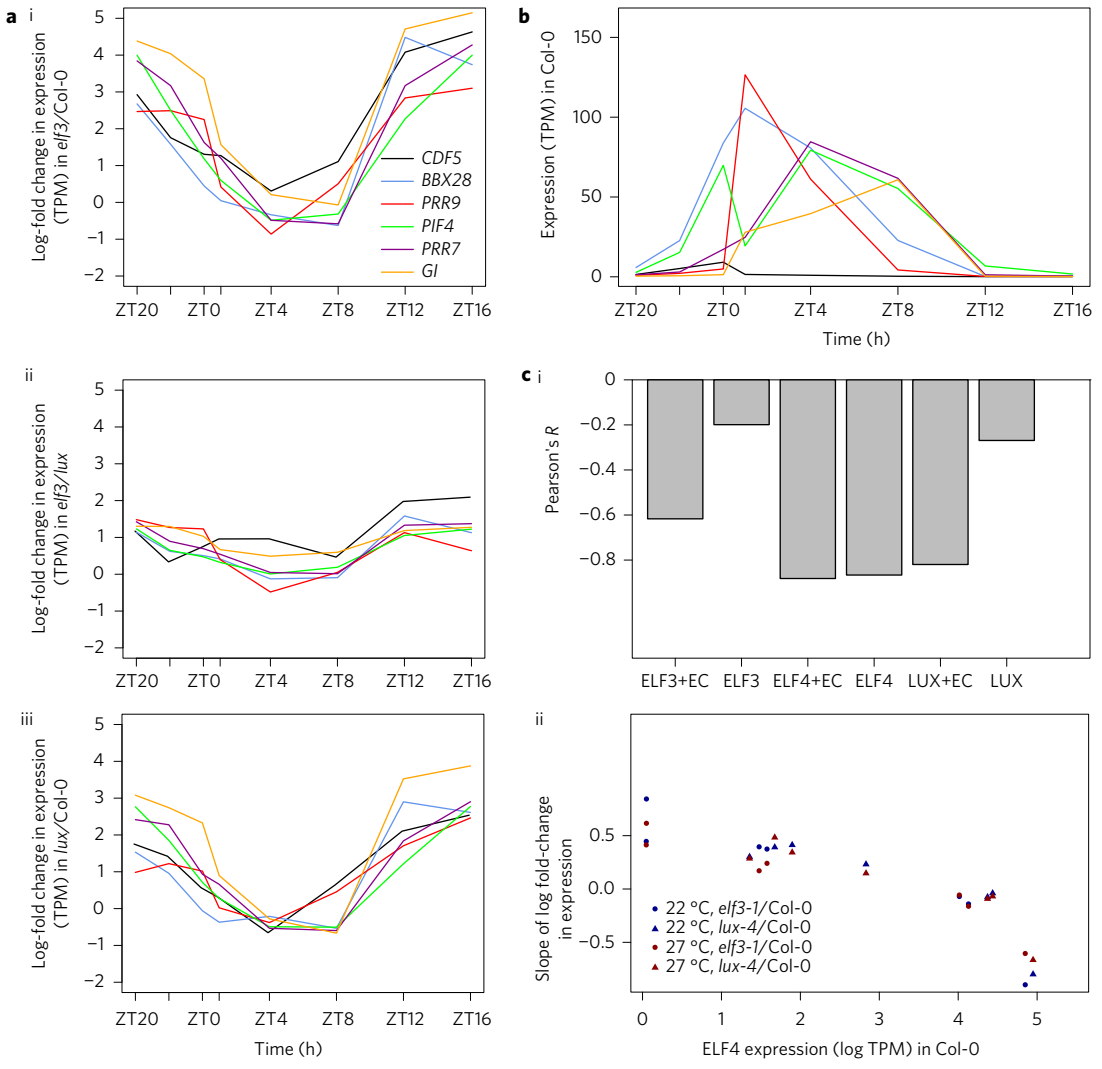

Figure 3 | The EC directly regulates many genes that are rhythmically expressed. a, The log-fold change in expression (natural log) is shown for *elf3-1* versus Col-0 (i), *elf3-1* versus *lux-4* (ii) and *lux-4* versus Col-0 (iii), specifically for the cluster containing circadian clock genes—indicated by purple in Fig. 2d. **b**, The expression (TPM) for these genes is shown in Col-0. Note that the legend is the same as in **a**. **c**, Six different models were fit to predict the slope of the change of expression of circadian target genes based on the expression of *ELF3, ELF4* or *LUX* (with or without dependence on a complete EC)—see Supplementary Fig. 9 for further explanation. More specifically, in the +EC models, we assume that the 'expression' of ELF3 is effectively zero in the absence of LUX (*lux-4*) and the 'expression' of LUX is effectively zero in the absence of ELF3 (*elf3-1*). For each of these models, we calculated the Pearson's correlation between the expression of each EC component and the slope of the log-fold change in expression in the genes shown in **a** (i). The results of the best model (using *ELF4* expression, dependent on complete EC) are also graphed (ii).

Fig. 2d. Firstly, we wished to determine whether these genes could be regulated by only the entire EC or whether LUX was capable of regulating these genes in the absence of ELF3. Figure 3a demonstrates that these genes have increased expression at night in both the *elf3-1* and *lux-4* backgrounds compared to Col-0, but that these genes have almost identical patterns of expression in *elf3-1* and *lux-4*. This suggests that both *LUX* and *ELF3* are required to regulate the circadian targets of the EC. Strikingly, even though the circadian targets have very distinctive gene expression patterns in Col-0 (Fig. 3b), they all have highly similar log-fold changes of expression in *elf3-1* and *lux-4* (Fig. 3a), suggesting that the EC provides the same degree of repression to all of its circadian targets. This indicates that the EC may act by a single mechanism, and that this repression is achieved independently of the other factors influencing expression of the target genes.

The genes encoding EC components show diurnal patterns of expression (Supplementary Fig. 12). We therefore investigated whether the expression of EC components is sufficient to account for the degree of EC target repression. As gene expression networks often assume that the concentration of a transcription factor influences the rate of change of gene expression of its downstream targets, we generated a set of linear models to predict the slopes of Fig. 3ai,iii based on the log-fold change in concentration of LUX, ELF3 or ELF4 (Supplementary Fig. 13). If we assume that all three EC components are required for EC function, the 'effective concentrations' of LUX in *elf3-1* and of ELF3 in *lux-4* should then both be zero—models that incorporate this assumption are labelled as +EC in Fig. 3ci. In all cases, models that incorporate this assumption perform better than ones that do not, further suggesting that both ELF3 and LUX must be present for the EC to serve as a repressor. The ELF4 and LUX + EC models were remarkably accurate—the Pearson's R values were less than −0.8 (Fig. 3ci). Therefore, the amount of repression of EC circadian targets can be accurately predicted using only information about either *LUX* or *ELF4* expression levels—an example of the correlation of the ELF4 + EC model is shown in Fig. 3cii. This suggests a quantitative model in

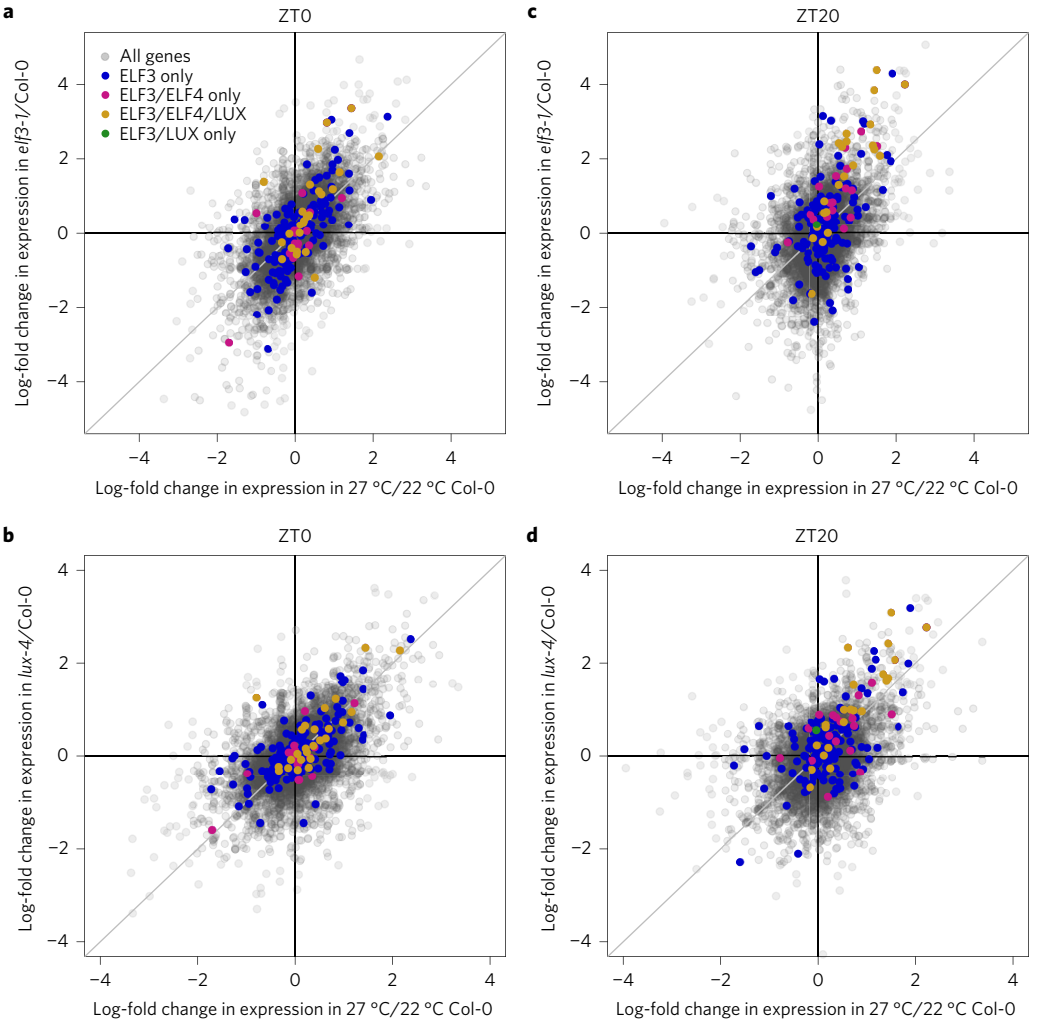

Figure 4 | The EC affects temperature response genome-wide. a,**b**, The log-fold change in expression caused by an elevated temperature (Col-0, 27 °C compared to 22 °C) is highly correlated with the log-fold change of expression in *elf3-1* (**a**), or *lux-4* (**b**) in 22 °C at ZT0 (immediately before lights are turned on) compared to Col-0 at 22 °C. **c**,**d**, Similar graphs are shown for ZT20, showing that EC targets show a warm temperature transcriptional pattern more clearly earlier in the night.

which the concentration of the EC determines the rate of repression of the circadian targets—a mechanism that could explain the expression of circadian targets at night. It is notable that the expression pattern of *ELF3* is very broad, with a much-reduced amplitude compared to that of *ELF4* and *LUX*, which show a very sharp peak of expression at ZT8 (Supplementary Fig. 12). Because *ELF4* and *LUX* have very similar patterns of expression, we cannot determine which is more important for circadian regulation using the modelling framework in Fig. 3. Finally, it is important to note that while this model is sufficient to explain our observations, the model may not be predictive.

The EC controls the night-time warm temperature transcriptome. The EC has been shown to control warm temperature-mediated induction of *PIF4* and *LUX* (ref. 15), and here we determined that the EC may also directly regulate key temperature response genes like *CBFs*. We therefore sought to see if the EC might play a global role in the warm temperature response. Comparing the transcriptomes of either *elf3-1* or *lux-4* with the warm temperature transcriptome reveals a significant positive correlation during the night (Fig. 4a,b, Supplementary Fig. 14, see "Scatterplot Stats" in Supplementary Table 3 for *P* value calculations). Interestingly, this correlation is stronger earlier in the night for those genes that are directly bound by the EC, while the correlation is strongest at the end of the night for all genes (Supplementary Fig. 14). This suggests that the EC conveys temperature information to its direct targets at night, and that this signal cascades to a wider set of genes by dawn (Fig. 4c,d, Supplementary Figs 14,15).

The EC associates with phytochromes on target gene promoters. To understand how the EC might integrate temperature information, we investigated other proteins that have been demonstrated to interact with the EC[30]. Of these, phytochromes have recently been shown to function as thermosensors[31,32], binding to target promoters in a temperature dependent manner. We therefore investigated whether the peaks bound by EC proteins are also bound by phytochromes. There is significant overlap between temperature responsive loci that are bound by two or more members of the EC and phyB (Fig. 5a, see "Fig. 5a" sheet in Supplementary Table 3 for *P* value calculations, Supplementary Table 8 for raw values and Supplementary Fig. 16 for specific examples). This suggests a mechanism whereby phytochromes may transmit light and temperature information directly to the evening expressed component of the clock.

Consistent with a direct role for phytochromes in controlling EC function, EC target genes have increased expression in *phyABCDE*

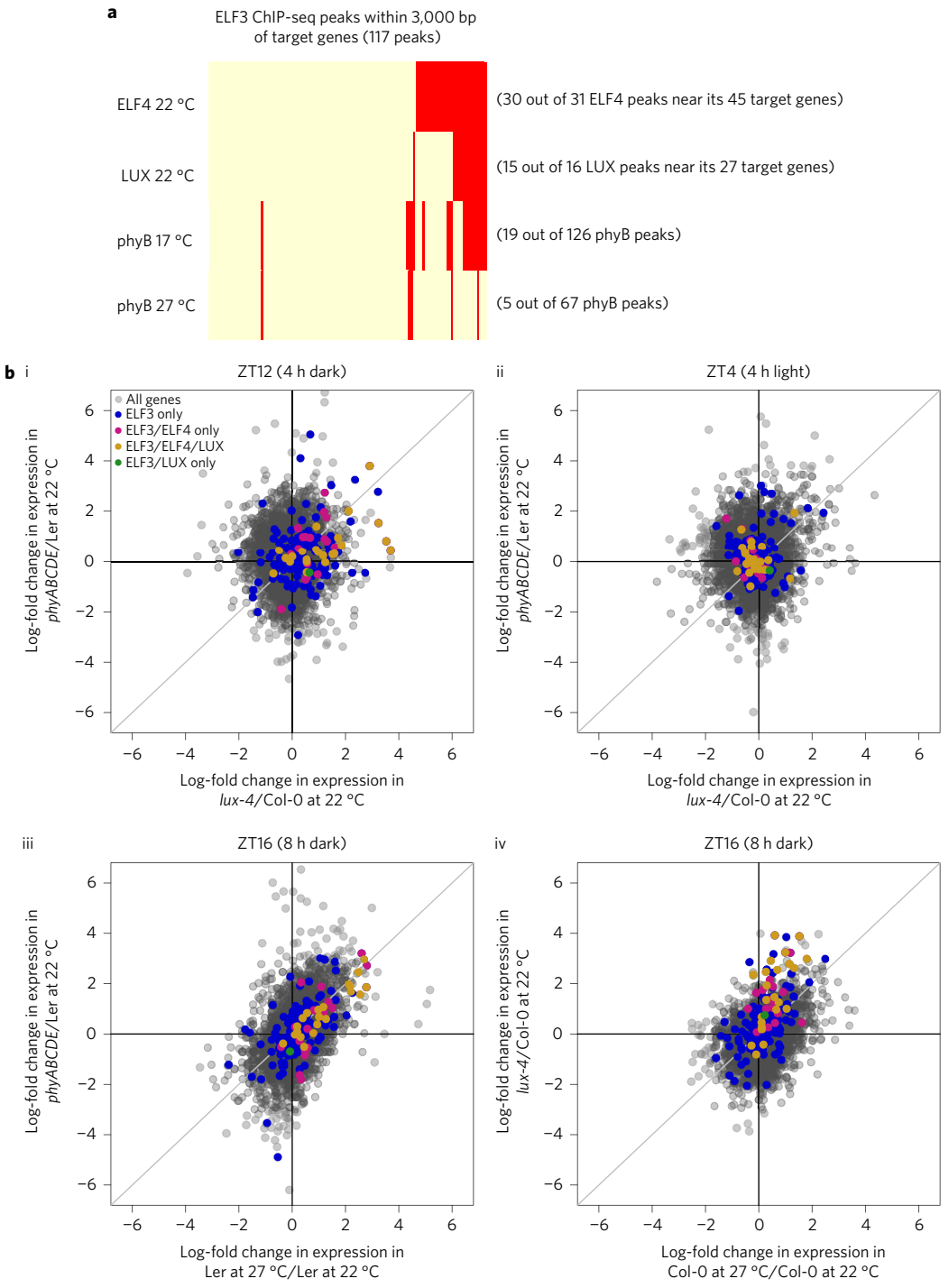

Figure 5 | EC target genes are temperature responsive. a, The binding sites of ELF3 overlap with those of ELF4, LUX and phyB (a red light and temperature sensor, data from ref. 31). Each column in this figure represents an ELF3 peak that is within 3,000 bp of a predicted target gene of ELF3—if the ELF3 peak overlaps with another ChIP-seq peak by at least one base pair, it is coloured red. **b**, The gene expression of the same set of genes used in Fig. 3a were compared, in a *phyABCDE* background and at different time points and temperatures. We compare the log-fold change of expression of *phyABCDE* (compared to Ler) in the early night (i) and day (ii), and also compare the log-fold change expression in *phyABCDE* versus Ler at 22 °C (iii) and *lux-4* versus Col-0 at 22 °C (iv) to the log-fold change in expression caused by a change in temperature—Ler (iii) and Col-0 (iv) at 27 °C versus 22 °C. Note that Jung *et al.*, 2016 did not conduct an RNA-sequencing on Ler at ZT12 at 27 °C, so the closest data point (ZT16) was used instead for iii–iv.

at night, but not in the day (Fig. 5bi,ii and Supplementary Fig. 14). Furthermore, EC targets have similar expression in *phyABCDE*, *elf3-1* and *lux-4* at 22 °C compared to wild type, as they do when the temperature is raised to 27 °C. Phytochromes not only colocalize with the EC, but they can also change the expression pattern of EC targets in a similar way as a change in temperature (Fig. 5biii,iv and Supplementary Fig. 14). A key question is whether the EC and phytochromes both relay temperature information, or whether a single component is sufficient. Since phyB is only detectable at a subset of the EC bound sites, and ELF4 targets do not completely lose their night-time temperature-dependent expression changes in either *lux-4* or *phyABCDE* (Supplementary Fig. 17), this suggests that both the EC

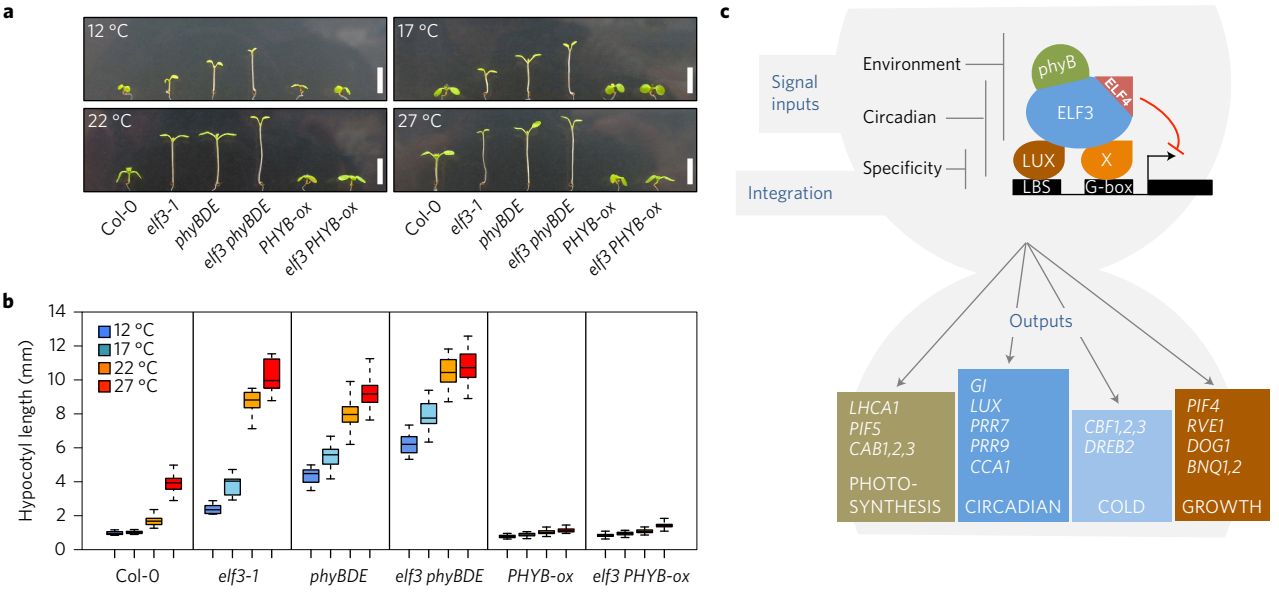

Figure 6 | The EC and phytochrome temperature response is additive in seedlings. a, Seedlings were grown at indicated temperatures for 7 days under short photoperiods. Scale bars, 5 mm. **b**, Hypocotyl length box plots for the indicated genotypes grown at different temperatures as in **a**. **c**, This model illustrates how EC integrates environmental and endogenous signals in plants. Note that ELF3 is sufficient for complex formation with LUX and ELF4[7]. Although there is an enrichment for G-boxes under EC binding sites, it is still not certain whether the G-box is necessary for EC binding. Additionally, recall that we could only find cobinding of phyB and the EC in a significant proportion—but not all—of the EC loci.

and phytochromes contribute to the temperature transcriptome. A candidate for the transmission of this temperature signal in the EC is ELF3, since even in the absence of LUX, ELF3 binding responds to temperature (Fig. 1d).

To understand the consequences and nature of the interactions between the EC and phytochromes with temperature, we analysed hypocotyl elongation, a phenotypic parameter that is very responsive to temperature. *elf3-1 phyBDE* quadruple mutants display greater hypocotyl elongation than either *elf3-1* or *phyBDE* seedlings, consistent with previous studies showing that *phyB* and *elf3* exhibit additive effects[33] (Fig. 6a,b). The difference between the *elf3-1* and *elf3-1 phyBDE* decreased at higher temperatures, which is expected since higher temperatures reduce the activity of both ELF3 and phytochromes. Interestingly, overexpressing *PHYB* is sufficient to largely abolish both the effect of *elf3-1* on hypocotyl elongation and thermal responsiveness. This is consistent with the role of phytochromes as thermosensors[31,32], and indicates that a sufficient level of phyB Pfr (the active state of phyB) can block growth regardless of temperature, presumably at least in part through directly inhibiting the action of PIF4 and PIF5. Taken together, these results indicate that phytochromes and the EC bind to common promoter binding sites, directly relaying temperature information to genes involved in growth and development.

Discussion

The circadian clock allows plants to anticipate changes and coordinate multiple processes, including photosynthesis, growth and temperature responses with the environment. The EC, a core component of the circadian clock, has been shown to be important in coordinating responses such as growth, but the underlying mechanism of action has not been clear. We have found that the EC achieves specificity of target binding through a combinatorial mechanism, requiring both LBS and G-box motifs to be present at functional sites. Since none of the core EC components have been described as having G-box binding activity, this suggests an additional transcription factor plays a key role in EC specificity. Interestingly, the bHLH transcription factor PIF7, which recognizes G-boxes, interacts with the EC in a phyB dependent manner[30]. Analysis of the *elf3-1* and *lux-4* transcriptomes enabled us to identify the set of high confidence direct EC functional target genes. This list reveals how extensively the EC is integrated into major transcriptional programmes in the cell, particularly photosynthesis, the circadian clock, growth, phytohormones and temperature signalling (Fig. 6b). Even in the *lux-4* background, we observe reduced but significant binding of ELF3 to EC targets, supporting a role for the related TF, BROTHER OF LUX ARRHYTHMO (BOA) within the EC[34]. Finally, EC function may also be controlled by post-translational mechanisms.

Not only is the EC able to coordinate the circadian regulation of thousands of transcripts by repressing targets in the early evening, but it also transmits temperature information to these genes. Indeed, we see direct EC targets are globally upregulated in *elf3-1* and *lux-4*, resembling a warm grown plant. This signal propagates over the course of the night, to affect the global transcriptome. Strikingly, we observe that the recently described thermosensor phyB is recruited to many EC loci. This suggests a direct mechanism whereby phyB Pfr (which also acts as a transcriptional repressor) may directly provide temperature and light information to the EC. The recruitment of phyB to large transcriptional complexes has recently been observed at the FLOWERING LOCUS T (FT) locus[35], suggesting this may represent a major mechanism for integrating environmental signals into gene expression. Consistent with previous observations[33], it appears that the interactions between *elf3-1* and phytochrome mutants are additive, and it is likely that additional temperature information is also transmitted by the EC. As well as cobinding to specific promoters, it is also apparent that the EC and phytochromes have independent functions, likely explaining their additive genetic interactions. It may seem contradictory that phytochromes and the EC interact physically, yet still display an additive phenotype. However, it is likely that the EC and phytochromes do not always function in complex—there are EC bound sites without phyB binding and vice versa. An intriguing line of future investigation would be to determine whether the EC and phytochromes influence each other's binding pattern—do these two components genetically interact by affecting each other's binding pattern or by affecting their activity? Environmental

temperature is a variable signal, and it may be that measuring it independently over multiple time-scales and integrating this information enables more robust decision-making. The EC has been shown to be central in controlling key agricultural traits[36], so understanding how this system transmits environmental information is particularly relevant during a period of climate change which threatens food security[37].

Methods

Plant material and growing methods. The *elf3-1 and lux-4* mutants have been described previously[15]. The *phyBDE* mutant in Columbia (Col) background was provided by P. Cerdán[38]. The *PHYB*-ox transgenic plant, in which the *PHYB-GFP* gene fusion is overexpressed in the *phyB-9* background, was obtained from F. Nagy[39]. An initial ChIP-seq experiment was conducted on *35S::cELF3-HA*—the CDS of ELF3 was cloned into pEG201 containing C-terminal HA tag and transformed into the *elf3-1* line, as described by Box *et al.*[15]. The *ELF3pro::ELF3-myc* transgenic plant (*ELF3-MYC*) was used in the remaining ChIP-seq experiments, and was constructed by amplifying a 7.8 kb genomic fragment of *ELF3* including its promoter with primers 6495 (5′-CACCGCTTCTTGTGTTAGTGACTTTCCTC) and 6497 (5′-AGGCTTAGAGGAGTCATAGCGTTTA). The PCR products were subcloned into pENTR vector (ThermoFisher) according to the manufacturer's procedure. The resultant entry plasmid was recombined with LR clonase into the Gateway binary pJHA212 K containing a C-terminal five copies of myc tag sequences. The binary construct was transformed into the *elf3-1* mutant by the floral dipping method. The *ELF3-MYC* transgenic plant was isolated by kanamycin selection and propagated to obtain single insertion lines rescuing the long hypocotyl phenotype of *elf3-1*. The complementation experiment for the *ELF3-MYC* line is shown in Supplementary Fig. 2. The *LUXpro::LUX-GFP lux-4* (*LUX-GFP*) and *ELF4pro::ELF4-HA elf4-2* (*ELF4-HA*) transgenic lines used for ChIP-seq experiments have been described previously[7]. The *LUX-GFP elf3-1* and *ELF3-MYC lux-4* were generated by crossing the *LUX-GFP* to the *elf3-1* and the *ELF3-MYC* to the *lux-4*, respectively. Their homozygous F3 generations were used for ChIP-seq experiments. *Arabidopsis* seeds were sterilized and sown on ½×Murashige and Skoog-agar (MS-agar) plates at pH 5.7 without sucrose. Sterilized seeds were stratified for 3 d at 4 °C in the dark and allowed to germinate for 24 h at 22 °C under cool-white fluorescent light at 170 µmol per m^2s. The plates were then transferred to short-day conditions (8 h light and 16 h dark) at different temperatures for assays.

ChIP-seq. Please note that the phyB ChIP-seq data used in Fig. 4 are previously published[31]. All ChIP-seq raw data is deposited in the NCBI Sequenced Read Archive (SRA) in PRJNA384110. The primary set of ChIP-seq experiments came from growing seedlings under short day (SD) conditions (8 h light, 16 h dark) on ½ MS agar plates without sucrose at constant 22 °C with samples collected at ZT10 (2 h after darkness). These are the primary ChIP-seq experiments analysed throughout the paper and there is only one replicate (Figs 1–4 and Supplementary Figs 3c (ZT10), 7–10, 14–16 and 17).

In order to determine whether temperature affected the stability of LUX, a temperature shift experiment was conducted under SD conditions in MS agar plates, in which plants were grown at 17 °C for 11 d and then a subset of these plants were shifted to 27 °C at the end of the light period (ZT8) and collected after 1 h or 2 h (ZT9 or ZT10), and control (constant 17 °C) plants were also collected from the same time points. Two replicates were conducted for this experiment. The experimental design of the temperature shift experiment is shown in Supplementary Fig. 1a and the results are in Supplementary Fig. 1b. The seedlings grown at constant 17 °C and collected at ZT10 are the ones shown in Fig. 1b and Fig. 2a,b, Supplementary Fig. 3 and Supplementary Fig. 10).

Also, to determine whether temperature affected the stability of ELF3, a temperature shift experiment was conducted in *ELF3-MYC* transgenic plants under SD conditions in ½ MS agar plates in which plants were grown at 22 °C at ZT8, and then a subset of these plants were shifted to 8 °C, 12 °C, 17 °C, 20 °C, 27 °C or 32 °C at ZT10 (Fig. 1c).

Next, to evaluate the consistency of EC binding sites across the time points of the RNA-sequencing (RNA-seq) experiment, a ChIP-seq was conducted on *ELF3-MYC* in SD conditions at constant 22 °C with plants harvested at ZT0, 4, 8, 12, 16 and 20. In addition, the *LUX-GFP* ChIP-seq was done for samples collected at ZT8 and ZT12 that were grown at constant 22 °C. Only one replicate was performed. The results are shown in Supplementary Fig. 3c,d.

Finally, to determine if LUX-GFP is capable of binding to DNA independent of ELF3, a *LUX-GFP* ChIP-seq was conducted in an *elf3-1* background at ZT8—only one replicate was performed, and these results are shown in Supplementary Fig. 4. Similarly, an *ELF3-MYC* ChIP-seq was performed in *lux-4* at ZT10 with one replicate (Fig. 1d).

In all of these ChIP-seq experiments, 3 g seedlings for each treatment were fixed under vacuum for 20 min in 1xPBS (10 mM PO_4^{3-}, 137 mM NaCl and 2.7 mM KCl) containing 1% formaldehyde (F8775, Sigma). The reaction was quenched by adding glycine to a final concentration of 62 mM. Chromatin immunoprecipitation (ChIP) was performed as described[40], with the exception that 100 µl of anti-c-Myc agarose affinity gel antibody was used (A7470, Sigma) per sample for seedlings expressing the appropriate epitope tagged protein. Monoclonal Anti-HA–Agarose (A2095, Sigma) for *ELF4-HA* seedlings, or GFP antibody from Abcam (ab290) with Dynabeads Protein A and G were used for immunoprecipitation of *LUX-GFP* seedlings. Sequencing libraries were prepared using TruSeq ChIP Sample Preparation Kit (Illumina IP-202-1024) or using NEBNext Ultra II DNA Library Prep Kit and samples were sequenced on either the Illumina HiSeq or the Illumina NextSequation 500 platforms, as indicated in our SRA submission.

ChIP-seq bioinformatics processing. A standard ChIP-seq bioinformatics pipeline was used to process the fastq files: reads were mapped to the TAIR10 *Arabidopsis* genome using bowtie2 (ref. 41), duplicate reads were removed, the reads were sorted and indexed using samtools[42] and finally the read counts were normalized to the genome-wide coverage. This pipeline is available on Github at https://github.com/ezer/EC.

Peaks were identified using MACS2 (ref. 43), using matching INPUT control samples. We used the following macs2 callpeak parameters for each ChIP-seq sample: "–keep-dup 1 –nomodel -p 0.05 –extsize <predictd>", where <predictd> is the estimated fragment size (using the macs2 predictd command). The returned peaks were further filtered using the following criteria: fold-change >5 (for 17 °C LUX data) or fold-change >3 (for everything else), and qvalue < 0.001. The 17 °C LUX data had many more peaks identified than the 22 °C even with the more stringent threshold for fold-change.

The Venn diagram for peak overlap was calculated using bedtools: "merge" was used to create a single bed file, and each bed file was intersected to this[44] (see Supplementary Fig. 18). There are fewer peaks in the Venn diagram than appear in our tables—if we observe two peaks of one transcription factor overlapping with a single peak in the other transcription factor, we will consider this to be a single peak overlapping event.

De novo motifs were predicted using Homer2 (ref. 45), using permuted sequence as background.

RNA-seq experiment. The Col-0, *elf3-1* and *lux-4* backgrounds were used for time-course RNA-seq experiments. Seedlings of the indicated genotypes were grown for 7 d at 22 °C and 27 °C and sampled at intervals over the diurnal cycle: ZT = 0, 1, 4, 8, 12, 16, 20 and 22 h. Total RNA was isolated from 30 mg of ground seedlings using the MagMAX-96 Total RNA Isolation kit (Ambion, AM1830), following the manufacturer's instructions. RNA quality and integrity was assessed on the Agilent 2200 TapeStation. Library preparation was performed using 1 µg of high integrity total RNA (RNA integrity number > 8) using the TruSeq RNA Library Preparation Kit v2 (Illumina, RS-122-2101 and RS-122-2001), following the manufacturer's instruction. The libraries were sequenced on a HiSeq2000 using paired-end sequencing of 100 bp in length at the Beijing Genomics Institute sequencing centre.

The same pipeline was used to map these sequences as described previously[31], with the exception that the sequences were mapped to the TAIR10 genome. To analyse the sequence reads: First, adapters were trimmed with Trimmomatic-0.32 (ref. 46). Then, Tophat[47] was used to map to the TAIR10 annotated genome, duplicates were removed and the read counts were normalized by genome-wide coverage. Raw counts were determined by HTseq-count[48], and cufflinks was used to calculate Fragments Per Kilobase Million, which was then converted into Transcripts Per Million (TPM). The RNA-seq data using the *phyABCDE* and Ler backgrounds, analysed in Fig. 4, were published previously[31].

All RNA-seq raw data is deposited in the NCBI SRA (PRJNA384110).

Identification of predicted target genes. All scripts used to identify predicted target genes are available in: https://github.com/ezer/EC. We predicted four distinct lists of prospective target genes (for LUX, ELF3 and ELF4 at 22 °C and for LUX at 27 °C) using the following criteria: (1) TAIR10 annotated genes that are within 3,000 bp of ChIP-seq peaks using bedmap and (2) that are within the top 5% most significant differentially expressed genes in at least one time point in either *elf3-1* vs. Col-0 or *lux-4* vs. Col-0, which was calculated using the edgeR (ref. 49) package, using raw read counts and the exactTest with dispersion 0.1.

Next, we could use this list of predicted target genes to annotate some of the ChIP-seq peaks as "high confidence peaks". These were peaks that were within 3,000 bp of genes that were on the prospective target gene lists. This strategy helped us filter out many of these peaks, which are likely false positives. GO analysis of our lists of predicted target genes was conducted using Panther (ref. 50) and goatools (ref. 51).

Analysis and modelling of log-fold change in expression. In all figures, log-fold change in expression refers to the natural logarithm of the TPM of the designated sample, minus the natural logarithm of the TPM in the associated wild type at 22 °C at the same time point. The associated wild type for *elf3-1* and *lux-4* is Col-0, while the associated wild type for *phyABCDE* is Ler. For instance, the log-fold change of expression in *lux-4* can be expressed as: $ln(TPM_{lux\text{-}4})$-$ln(TPM_{Col\text{-}0})$.

All of the plots related to log-fold change in expression were drawn in R. All of the hierarchical clustering uses default parameters from heatmap.2. Note that the heatmap in Supplementary Fig. 11 uses z-scores of the TPM, rather than log-fold change in expression.

We also attempt to determine whether it is possible to predict the rate of repression of the EC from the expression of EC components—the problem statement is described in more depth in Supplementary Fig. 13. The models were fit by least-squares regression (lm in R). Note that since the slope is calculated across two points and there are four time-course experiments with eight time points each, there are a total of 28 data-points (seven slopes per time-course). Since this is a small number of points, we decided that each model should not have more than one fitted parameter, to decrease the likelihood of over-fitting our data. Also note that for each time-course experiment there are eight collection time points (and therefore eight LUX, ELF4 or ELF3 concentrations per time course), but only seven slopes: because of this, we chose to take the average TPM value between every consecutive pair of collection points.

Hypocotyl length measurements. To examine how phytochrome and EC signalling pathways interact for the thermal regulation of hypocotyl elongation, the *phyBDE* and *PHYB*-ox were crossed with *elf3-1* and the resultant homozygous F3 generations were used for hypocotyl length measurements at different temperatures, as described previously[15]. Seedlings, which were grown for 8 d under SD conditions with light intensity of 80 μmol per m^2s, were photographed and analysed using ImageJ software (http://rsbweb.nih.gov/ij/).

Western blots. Seedlings were surface sterilized and grown on plates (0.5×Murashige and Skoog, 0.7% agar) for 10 d under short-day conditions (8 h light/16 h dark) in Panasonic growth chambers. Proteins were extracted and separated by SDS-PAGE and transferred to PVDF membrane using Trans-Blot Turbo Transfer System (Bio-Rad). ELF4 was detected using HA antibody coupled to horse radish peroxidase (HRP) (1:500, 12013819001, Roche), LUX using mouse anti-GFP (1:1,000, 632380, Clontech Laboratories) and ELF3 using mouse anti-myc (1:10,00, 05-724, Millipore), and secondary goat derived anti-mouse conjugated to HRP (1:3,000, sc-2005, Santa Cruz Biotechnology). PVDF membranes were developed using Pierce ECL western blotting substrate (32106, Thermo Scientific), and scanned using an Amersham Imager 600 (GE Healthcare Life Sciences). Loading controls were obtained by staining membranes with Ponceau S solution (P7170, Sigma).

Detailed experimental set up is described below for each line used.

(1) (a) The *LUX-GFP elf3-1* transgenic seedlings were grown continuously at 22 °C or 27 °C and harvested at ZT12. Aliquots for western blot analysis were taken during chromatin immunoprecipitation (ChIP) preparation; (b) The *LUX-GFP* transgenic seedlings were grown at 17 °C and harvested at ZT8 or for second collection point seedlings were shifted on rafts to 27 °C or kept at 17 °C and harvested at ZT10. Nuclei enriched samples were prepared as for ChIP and loaded with SDS buffer. (2) The *ELF3-MYC* and *ELF3-MYC lux-4* transgenic seedlings were grown at 22 °C, sampled and shifted at ZT8 to 27 °C or kept at 22 °C and sampled at ZT10. Aliquots for western blot analysis were taken during ChIP preparation. (3) The *ELF4-HA* transgenic seedlings were grown at 22 °C and shifted at ZT8 to 27 °C or kept at 22 °C and sampled at ZT10 and whole plant extract was ground in SDS buffer and supernatant loaded. (4) The *PHYBpro::PHYB-myc phyB-9* (*PHYB-MYC*) transgenic seedlings were grown at 17 °C and harvested at ZT8; for second collection points seedlings were shifted on rafts to 27 °C or kept at 17 °C and harvested at ZT10 and whole plant material after grinding was boiled in SDS buffer and supernatant loaded. (5) The *ELF3-MYC* transgenic seedlings were grown at 17 °C and harvested at ZT8; for second collection points seedlings were shifted on rafts to 27 °C or kept at 17 °C and harvested at ZT10 and whole plant extract was boiled in SDS buffer and the supernatant loaded. Col-0 was added as negative control in all western blots.

Statistical tests. In all cases where statistical tests are used in the text, a Fisher exact test is applied using R and either a Bonforroni or Holms–Bonferroni correction for multiple hypothesis testing is used as described in Supplementary Table 3.

Data Availability. All data is available in SRA (PRJNA384110). All code used to generate the figures is available on github (https://github.com/ezer/EC).

Received 29 September 2016; accepted 12 May 2017; published 26 June 2017

References

1. Willis, C. G., Ruhfel, B., Primack, R. B., Miller-Rushing, A. J. & Davis, C. C. Phylogenetic patterns of species loss in Thoreau's woods are driven by climate change. *Proc. Natl Acad. Sci. USA* **105,** 17029–17033 (2008).
2. Fitter, A. H. & Fitter, R. S. Rapid changes in flowering time in British plants. *Science* **296,** 1689–1691 (2002).
3. Dodd, A. N. *et al.* Plant circadian clocks increase photosynthesis, growth, survival, and competitive advantage. *Science* **309,** 630–633 (2005).
4. Harmer, S. L. *et al.* Orchestrated transcription of key pathways in *Arabidopsis* by the circadian clock. *Science* **290,** 2110–2113 (2000).
5. Huang, H. & Nusinow, D. A. Into the evening: complex interactions in the *Arabidopsis* circadian clock. *Trends Genet.* https://dx.doi.org/10.1016/j.tig.2016.08.002 (2016).
6. Greenham, K. & McClung, C. R. Integrating circadian dynamics with physiological processes in plants. *Nat. Rev. Genet.* **16,** 598–610 (2015).
7. Nusinow, D. A. *et al.* The ELF4-ELF3-LUX complex links the circadian clock to diurnal control of hypocotyl growth. *Nature* **475,** 398–402 (2011).
8. Thines, B. & Harmon, F. G. Ambient temperature response establishes ELF3 as a required component of the core *Arabidopsis* circadian clock. *Proc. Natl Acad. Sci. USA* **107,** 3257–3262 (2010).
9. Filo, J. *et al.* Gibberellin driven growth in *elf3* mutants requires PIF4 and PIF5. *Plant Signal. Behav.* **10,** e992707 (2015).
10. Koini, M. A. *et al.* High temperature-mediated adaptations in plant architecture require the bHLH transcription factor PIF4. *Curr. Biol.* **19,** 408–413 (2009).
11. Kumar, S. V. *et al.* Transcription factor PIF4 controls the thermosensory activation of flowering. *Nature* **484,** 242–245 (2012).
12. Thines, B. C., Youn, Y., Duarte, M. I. & Harmon, F. G. The time of day effects of warm temperature on flowering time involve PIF4 and PIF5. *J. Exp. Bot.* **65,** 1141–1151 (2014).
13. Fernández, V., Takahashi, Y., Le Gourrierec, J. & Coupland, G. Photoperiodic and thermosensory pathways interact through CONSTANS to promote flowering at high temperature under short days. *Plant J.* **86,** 426–440 (2016).
14. Sureshkumar, S., Dent, C., Seleznev, A., Tasset, C. & Balasubramanian, S. Nonsense-mediated mRNA decay modulates FLM-dependent thermosensory flowering response in *Arabidopsis*. *Nat. Plants* **2,** 16055 (2016).
15. Box, M. S. *et al.* ELF3 controls thermoresponsive growth in *Arabidopsis*. *Curr. Biol.* **25,** 194–199 (2015).
16. Raschke, A. *et al.* Natural variants of ELF3 affect thermomorphogenesis by transcriptionally modulating PIF4-dependent auxin response genes. *BMC Plant Biol.* **15,** 197 (2015).
17. Helfer, A. *et al.* LUX ARRHYTHMO encodes a nighttime repressor of circadian gene expression in the *Arabidopsis* core clock. *Curr. Biol.* **21,** 126–133 (2011).
18. Chow, B. Y., Helfer, A., Nusinow, D. A. & Kay, S. A. ELF3 recruitment to the PRR9 promoter requires other evening complex members in the *Arabidopsis* circadian clock. *Plant Signal. Behav.* **7,** 170–173 (2012).
19. Yu, C.-P., Lin, J.-J. & Li, W.-H. Positional distribution of transcription factor binding sites in *Arabidopsis thaliana*. *Sci. Rep.* **6,** 25164 (2016).
20. O'Malley, R. C. *et al.* Cistrome and epicistrome features shape the regulatory DNA landscape. *Cell* **165,** 1280–1292 (2016).
21. Mizuno, T. *et al.* Ambient temperature signal feeds into the circadian clock transcriptional circuitry through the EC night-Time repressor in *Arabidopsis thaliana*. *Plant Cell Physiol.* **55,** 958–976 (2014).
22. Hsu, P. Y. & Harmer, S. L. Wheels within wheels: the plant circadian system. *Trends Plant Sci.* **19,** 240–249 (2014).
23. Mochizuki, N., Brusslan, J. A., Larkin, R., Nagatani, A. & Chory, J. *Arabidopsis* genomes uncoupled 5 (GUN5) mutant reveals the involvement of Mg-chelatase H subunit in plastid-to-nucleus signal transduction. *Proc. Natl Acad. Sci. USA* **98,** 2053–2058 (2001).
24. Cheng, N.-H., Liu, J.-Z., Brock, A., Nelson, R. S. & Hirschi, K. D. AtGRXcp, an *Arabidopsis* chloroplastic glutaredoxin, is critical for protection against protein oxidative damage. *J. Biol. Chem.* **281,** 26280–8 (2006).
25. Chow, B. Y. *et al.* Transcriptional regulation of LUX by CBF1 mediates cold input to the circadian clock in *Arabidopsis*. *Curr. Biol.* **24,**, (2014).
26. Bai, M.-Y., Fan, M., Oh, E. & Wang, Z.-Y. A triple helix-loop-helix/basic helix-loop-helix cascade controls cell elongation downstream of multiple hormonal and environmental signaling pathways in *Arabidopsis*. *Plant Cell* **24,** 4917–4929 (2012).
27. Ikeda, M., Fujiwara, S., Mitsuda, N. & Ohme-Takagi, M. A triantagonistic basic helix-loop-helix system regulates cell elongation in *Arabidopsis*. *Plant Cell* **24,** 4483–4497 (2012).
28. Rawat, R. *et al.* REVEILLE1, a Myb-like transcription factor, integrates the circadian clock and auxin pathways. *Proc. Natl Acad. Sci. USA* **106,** 16883–8 (2009).
29. Nitschke, S. *et al.* Circadian stress regimes affect the circadian clock and cause jasmonic acid-dependent cell death in cytokinin-deficient *Arabidopsis* plants. *Plant Cell* **28,** 1616–1639 (2016).
30. Huang, H. *et al.* Identification of evening complex associated proteins in *Arabidopsis* by affinity purification and mass spectrometry. *Mol. Cell. Proteomics* **15,** 201–217 (2016).
31. Jung, J.-H. *et al.* Phytochromes function as thermosensors in *Arabidopsis*. *Science* **354,** 886–889 (2016).
32. Legris, M. *et al.* Phytochrome B integrates light and temperature signals in *Arabidopsis*. *Science* **354** 897–900 (2016).
33. Reed, J. W. *et al.* Independent action of ELF3 and phyB to control hypocotyl elongation and flowering time. *Plant Physiol.* **122,** 1149–1160 (2000).
34. Dai, S. *et al.* BROTHER OF LUX ARRHYTHMO is a component of the *Arabidopsis* circadian clock. *Plant Cell* **23,** 961–972 (2011).
35. Kaiserli, E. *et al.* Integration of light and photoperiodic signaling in transcriptional nuclear foci. *Dev. Cell* **35,** 311–321 (2015).

36. Bendix, C., Marshall, C. M. & Harmon, F. G. Circadian clock genes universally control key agricultural traits. *Mol. Plant* **8,** 1135–1152 (2015).
37. Battisti, D. S. & Naylor, R. L. Historical warnings of future food insecurity with unprecedented seasonal heat. *Science* **323,** 240–244 (2009).
38. Strasser, B., Sanchez-Lamas, M., Yanovsky, M. J., Casal, J. J. & Cerdan, P. D. *Arabidopsis thaliana* life without phytochromes. *Proc. Natl Acad. Sci. USA* **107,** 4776–4781 (2010).
39. Medzihradszky, M. *et al.* Phosphorylation of phytochrome B inhibits light-induced signaling via accelerated dark reversion in *Arabidopsis*. *Plant Cell* **25,** 535–544 (2013).
40. Jaeger, K. E., Pullen, N., Lamzin, S., Morris, R. J. & Wigge, P. A. Interlocking feedback loops govern the dynamic behavior of the floral transition in *Arabidopsis*. *Plant Cell* **25,** 820–833 (2013).
41. Langmead, B. & Salzberg, S. L. Fast gapped-read alignment with bowtie 2. *Nat. Methods* **9,** 357–359 (2012).
42. Li, H. *et al.* The sequence alignment/Map format and SAMtools. *Bioinformatics* **25,** 2078–2079 (2009).
43. Zhang, Y. *et al.* Model-based analysis of ChIP-Seq (MACS). *Genome Biol.* **9,** R137 (2008).
44. Quinlan, A. R. & Hall, I. M. BEDTools: a flexible suite of utilities for comparing genomic features. *Bioinformatics* **26,** 841–842 (2010).
45. Heinz, S. *et al.* Simple combinations of lineage-determining transcription factors prime cis-regulatory elements required for macrophage and B cell identities. *Mol. Cell* **38,** 576–589 (2010).
46. Bolger, A. M., Lohse, M. & Usadel, B. Trimmomatic: a flexible trimmer for illumina sequence data. *Bioinformatics* **30,** 2114–2120 (2014).
47. Trapnell, C., Pachter, L. & Salzberg, S. L. Tophat: discovering splice junctions with RNA-seq. *Bioinformatics* **25,** 1105–1111 (2009).
48. Anders, S., Pyl, P. T. & Huber, W. HTSeq–a python framework to work with high-throughput sequencing data. *Bioinformatics* **31,** 166–169 (2015).
49. Robinson, M. D., McCarthy, D. J. & Smyth, G. K. Edger: a bioconductor package for differential expression analysis of digital gene expression data. *Bioinformatics* **26,** 139–140 (2010).
50. Mi, H., Muruganujan, A., Casagrande, J. T. & Thomas, P. D. Large-scale gene function analysis with the PANTHER classification system. *Nat. Protoc.* **8,** 1551–1566 (2013).
51. Tang, H. *et al.* GAOTOOLS: Tools for Gene Ontology. Zenodo. http://dx.doi.org/10.5281/zenodo.31628 (2015).
52. Jansson. A guide to the Lhc genes and their relatives in *Arabidopsis*. *Trends Plant Sci.* **4,** 236–240 (1999).
53. Hornitschek, P. *et al.* Phytochrome interacting factors 4 and 5 control seedling growth in changing light conditions by directly controlling auxin signaling. *Plant J.* **71,** 699–711 (2012).
54. Mitra, A., Choi, H. K. & An, G. Structural and functional analyses of *Arabidopsis thaliana* chlorophyll a/b-binding protein (cab) promoters. *Plant Mol. Biol.* **12,** 169–179 (1989).
55. Beligni, M. V. & Mayfield, S. P. *Arabidopsis thaliana* mutants reveal a role for CSP41a and CSP41b, two ribosome-associated endonucleases, in chloroplast ribosomal RNA metabolism. *Plant Mol. Biol.* **67,** 389–401 (2008).
56. Park, D. H. *et al.* Control of circadian rhythms and photoperiodic flowering by the *Arabidopsis* GIGANTEA gene. *Science* **285,** 1579–82 (1999).
57. Salome, P. A. & McClung, C. R. PSEUDO-RESPONSE REGULATOR 7 and 9 are partially redundant genes essential for the temperature responsiveness of the *Arabidopsis* circadian clock. *Plant Cell* **17,** 791–803 (2005).
58. Salome, P. A., Weigel, D. & McClung, C. R. The role of the *Arabidopsis* morning loop components CCA1, LHY, PRR7, and PRR9 in temperature compensation. *PLANT CELL ONLINE* **22,** 3650–3661 (2010).
59. Seung, D. *et al. Arabidopsis thaliana* AMY3 is a unique redox-regulated chloroplastic α-amylase. *J. Biol. Chem.* **288,** 33620–33 (2013).
60. Seaton, D. D. *et al.* Linked circadian outputs control elongation growth and flowering in response to photoperiod and temperature. *Mol. Syst. Biol.* **11,** 776 (2015).
61. Jaglo-Ottosen, K. R., Gilmour, S. J., Zarka, D. G., Schabenberger, O. & Thomashow, M. F. *Arabidopsis* CBF1 overexpression induces COR genes and enhances freezing tolerance. *Science* **280,** 104–106 (1998).
62. Riechmann, J. L. *et al. Arabidopsis* transcription factors: genome-wide comparative analysis among eukaryotes. *Science* **290,** 2105–2110 (2000).
63. Chen, K.-M. *et al.* Small chloroplast-targeted DnaJ proteins are involved in optimization of photosynthetic reactions in *Arabidopsis thaliana*. *BMC Plant Biol.* **10,** 43 (2010).
64. Kendall, S. L. *et al.* Induction of dormancy in *Arabidopsis* summer annuals requires parallel regulation of DOG1 and hormone metabolism by low temperature and CBF transcription factors. *Plant Cell* **23,** 2568–80 (2011).
65. Wang, H. *et al.* Regulation of *Arabidopsis* brassinosteroid signaling by atypical basic helix-loop-helix proteins. *Plant Cell* **21,** 3781–3791 (2009).
66. Crocco, C. D. *et al.* The transcriptional regulator BBX24 impairs DELLA activity to promote shade avoidance in *Arabidopsis thaliana*. *Nat. Commun.* **6,** 6202 (2015).
67. Gangappa, S. N. *et al.* The *Arabidopsis* B-BOX protein BBX25 interacts with HY5, negatively Regulating BBX22 expression to suppress seedling photomorphogenesis. *Plant Cell* **25,** 1243–1257 (2013).
68. Bartrina, I., Otto, E., Strnad, M., Werner, T. & Schmülling, T. Cytokinin regulates the activity of reproductive meristems, flower organ size, ovule formation, and thus seed yield in *Arabidopsis thaliana*. *Plant Cell* **23,** 69–80 (2011).
69. Zwack, P. J. & Rashotte, A. M. Interactions between cytokinin signalling and abiotic stress responses. *J. Exp. Bot.* **66,** 4863–4871 (2015).
70. Cutcliffe, J. W., Hellmann, E., Heyl, A. & Rashotte, A. M. CRFs form protein–protein interactions with each other and with members of the cytokinin signalling pathway in *Arabidopsis* via the CRF domain. *J. Exp. Bot.* **62,** 4995–5002 (2011).
71. Zwack, P. J. *et al.* Cytokinin response factor 6 represses cytokinin-associated genes during oxidative stress. *Plant Physiol.* **172,** pp. 00415.2016 (2016).
72. Wilson, M. E., Mixdorf, M., Berg, R. H. & Haswell, E. S. Plastid osmotic stress influences cell differentiation at the plant shoot apex. *Development* **143,** 3382–93 (2016).
73. Rawat, R. *et al.* REVEILLE1, a Myb-like transcription factor, integrates the circadian clock and auxin pathways. *Proc. Natl Acad. Sci. USA* **106,** 16883–8 (2009).
74. Dong, T. *et al.* Abscisic Acid uridine diphosphate glucosyltransferases play a crucial role in abscisic acid homeostasis in *Arabidopsis*. *Plant Physiol.* **165,** 277–289 (2014).
75. Rizza, A., Boccaccini, A., Lopez-Vidriero, I., Costantino, P. & Vittorioso, P. Inactivation of the ELIP1 and ELIP2 genes affects *Arabidopsis* seed germination. *New Phytol.* **190,** 896–905 (2011).
76. Li, G. *et al.* Coordinated transcriptional regulation underlying the circadian clock in *Arabidopsis*. *Nat. Cell Biol.* **13,** 616–622 (2011).

Acknowledgements

We thank members of the Wigge laboratory for feedback and discussions. This work was supported by the Biotechnology and Biology Research Council (RG80054 to P.A.W.); P.A.W.'s laboratory is supported by a Fellowship from the Gatsby Foundation (GAT3273/GLB). Funding for open access charge: (Gatsby Foundation/GAT3273/GLB). We thank S. Kay for providing us with the gLUX-GFP *lux-4* and gELF4-HA *elf4-2* transgenic plants.

Author contributions

D.E.: wrote a large proportion of the manuscript, lead researcher on all analysis. Involved in experimental design, prepared Figs 1–4. J.-H.J.: experimental design, generated Fig. 5, created lines used in the study. H.L.: extensive bioinformatics analysis. Mapped and analysed most of the datasets for the ChIP experiments. Performed motif searching and so on. S.B.: performed the initial mapping of the first ELF3 ChIP and made insights into rhythmical gene expression using clustering that were instrumental in the development of the project. L.G.: collaborating group. Performed the first analysis of EC binding and motif analysis. M.S.B.: generated the RNA-seq time course datasets. V.C.: generated the RNA-seq time course datasets. S.C.: generated the RNA-seq time course datasets. D.S.: helped perform ChIP-seq experiments. C.Z.: PI. Collaborator, supervisor of L.G., made key structural biology and experimental design contributions. Helped write the paper. K.E.J.: PI. Performed all the ChIP-seq experiments the paper is based on. Writing the paper and experimental design. P.A.W.: PI. Experimental design and discussions, helped write the paper.

Additional information

Supplementary information is available for this paper.

Reprints and permissions information is available at www.nature.com/reprints.

Correspondence and requests for materials should be addressed to P.A.W.

How to cite this article: Ezer, D. *et al.* The evening complex coordinates environmental and endogenous signals in *Arabidopsis*. *Nat. Plants* **3,** 17087 (2017).

Publisher's note: Springer Nature remains neutral with regard to jurisdictional claims in published maps and institutional affiliations.

Competing interests

The authors declare no competing financial interests.